Efficient Intramolecular Charge Transfer in Oligoyne-Linked D–π–A Molecular Wires

Lars-Olof Pålsson,*,† Changsheng Wang,† Andrei S. Batsanov,† Simon M. King,‡ Andrew Beeby,† Andrew P. Monkman‡ and Martin R. Bryce*,†

Contribution from the Department of Chemistry and the Department of Physics, Durham University, Durham DH1 3LE, UK

Received: ; E-mails: m.r.bryce@durham.ac.uk; lars-olof.palsson@durham.ac.uk

***Abstract**:* **Studies are reported on a series of triphenylamine–$(C\equiv C)_n$–2,5-diphenyl-1,3,4-oxadiazole dyad molecules (1, 2, 3 and 4; *n* = 1-4, respectively) and the related triphenylamine–C_6H_4–$(C\equiv C)_3$–oxadiazole dyad 5. The oligoyne-linked D–π–A dyad systems have been synthesized by palladium-catalyzed cross-coupling of terminal alkynyl and butadiynyl synthons with the corresponding bromoalkynyl moieties. Cyclic voltammetric studies reveal a reduction in the HOMO-LUMO gap in the series of compounds 1–4 as the oligoyne chain length increases which is consistent with extended conjugation through the elongated bridges. Photophysical studies provide new insights into conjugative effects in oligoyne molecular wires. In non-polar solvents the emission from these dyad systems has two different origins: a locally excited (LE) state which is responsible for a $\pi^* \rightarrow \pi$ fluorescence and an intramolecular charge transfer (ICT) state which produces charge transfer emission. In polar solvents the LE state emission vanishes and only ICT emission is observed. This emission displays strong solvatochromism and analysis according to the Lippert-Mataga-Oshika formalism shows significant ICT for all the luminescent compounds with high efficiency even for the longer more conjugated systems. The excited state properties of the dyads in non-polar solvents vary with the extent of conjugation. For more conjugated systems a fast non-radiative route dominates the excited state decay and follows the Engelman-Jortner energy gap law. The data suggest that the non-radiative decay is driven by the weak coupling limit.**

Introduction

Charge and electron transfer dynamics through organic molecular wires are of major interest in chemistry, physics and biology.[1] Important incentives for studying this topic stem from both fundamental and practical aspects, in particular: (i) the development of new materials for the emerging technologies of molecular and nanoscale electronics,[2] and (ii) understanding and mimicking key biological molecules which mediate electron transfer processes, e.g. photosynthetic reaction centers, redox proteins and nucleic acids.[3] Many successful strategies have been developed to control and tune the magnitude of charge transfer through conjugated bridges by end-capping with various organic donor and acceptor groups, i.e. covalent D–π–A systems (D = electron donor; A = electron acceptor)[4] or organometallic moieties.[5] In these molecules the systematic variation of parameters such as the redox potentials of the end groups, free energy changes in charged states, intramolecular distances (i.e. length of the bridge), topology and relative orientations of the component units has enabled charge separation and storage characteristics to be probed in great detail by electrochemical and spectroscopic techniques. On the basis of this information, organic molecules - including oligomers and polymers[6] - can now be tailored for specific electrical or optoelectronic applications, such as wires,[7] switches,[8] photovoltaic cells,[9] electroluminescent devices,[10] field effect transistors[11] and single-molecule electrode junctions.[12]

To enhance electronic communication over nanometer distances, conjugated D–π–A dyad systems which possess delocalized π–systems and tunable HOMO-LUMO gaps are attractive targets. With sufficient overlap between the wave functions, electron transfer along the wire can be facilitated. In this context, a range of conjugated π-electron bridges have been studied. Specific examples include: oligo(*para*-phenylene)s,[13] oligo(*para*-phenylenevinylene)s (OPVs),[14] oligo(*para*-phenyleneethynylene)s (OPEs),[15] oligofluorenes,[16] oligothiophenes,[17] oligoenes and carotenoids.[18]

Oligoynes [(C≡C–)$_n$] comprise an array of *sp*-hybridized carbon atoms with approximately cylindrical electron delocalization along a one-dimensional, rigid-rod backbone[19] and they have only rarely been studied as bridges in organic D–π–A systems. This is largely due to the significant synthetic challenges posed by unsymmetrical derivatives with $n > 2$.[19d,e] To our knowledge, the only previous

systematic study concerns a series of Zn-porphyrin–$(C\equiv C)_n$–C_{60} dyads (n = 1-4) in which photoinduced charge separation and charge recombination were studied as a function of D–A distance.[20] The observed very efficient electron transfer [small attenuation factor (β) of 0.06 ± 0.005 $Å^{-1}$] was rationalized in terms of full π-conjugation between the phenyl ring of the porphyrin donor, the oligoyne linker and the C_{60} acceptor. Oligoynes are linear structures through which electron transport is independent of rotation around the single bonds – a feature which makes them clearly distinct from OPVs and OPEs, where the barrier to rotation around single bonds is low and conjugation is interrupted when the phenyl rings are rotated with respect to each other.[21] Previous experimental studies of the optical properties of symmetrical silyl end-capped oligoynes (n = 2 – 10) established that they possess extensive conjugation which was supported by theoretical models of the third-order nonlinear optical response as a function of the number of alkyne units.[22]

We recently described compounds **1** and **2** as part of a study on D–π–A dyads with different electron donor moieties [D = tetrathiafulvalene (TTF), bithiophene, 9-(4,5-dimethyl-1,3-dithiol-2-ylidene)fluorene and triphenylamine] connected to electron-accepting 2,5-diphenyl-1,3,4-oxadiazole (OXD) units. The latter was chosen because of its excellent chemical and thermal stabilities and high photoluminescence quantum yield (PLQY). We established that both **1** and **2** are strongly luminescent although the PLQY was lower for **2** and it was concluded that intramolecular energy transfer was less efficient through the butadiynylene bridge (**2**) than the ethynylene bridge (**1**).[23] Based on these initial results, we have now focused our attention on a more extensive series of triphenylamine–$(C\equiv C)_n$–2,5-diphenyl-1,3,4-oxadiazole molecules including novel hexatriyne and octatetrayne analogs [series **1**, **2**, **3** and **4** (n = 1-4, respectively) and the related triphenylamine–C_6H_4–$(C\equiv C)_3$–diphenyloxadiazole **5**] with the aim of probing their optoelectronic properties as a function of D–A distance. This work provides new insights into conjugative effects of oligoyne bridges and, in particular, establishes that non-radiative decay in oligoynes follows the Engelman-Jortner energy gap law.[24]

Results and Discussion

Chart 1. Structures of the oligoyne-linked dyads used in this study.

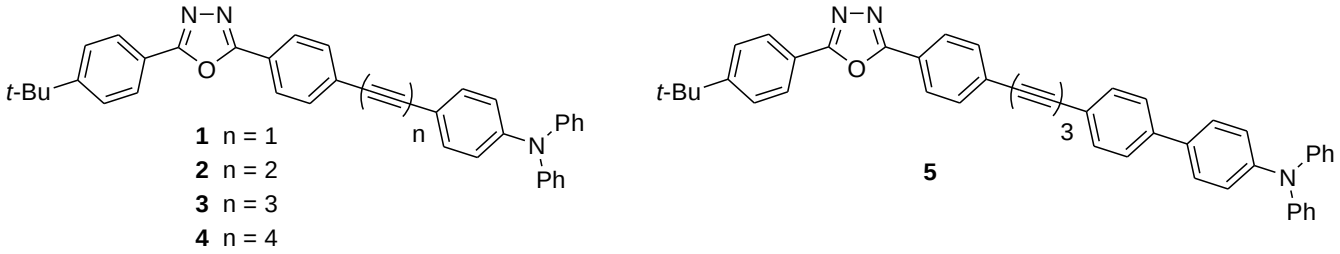

Synthesis. The general protocol for synthesizing the molecules **1**-**5** shown in Chart 1 involved palladium-catalyzed cross-coupling reactions of terminal alkynes with terminal alkynyl bromides. Compound **6** reacted with 1-bromo-2-trimethylsilylacetylene (TMSA bromide) to give compound **7** which was desilylated using potassium carbonate in MeOH-CH_2Cl_2 at room temperature to give the terminal butadiyne reagent **8** which was isolated as a crystalline solid (Scheme 1, 35% overall yield for the two steps).

Scheme 1. Synthesis of terminal butadiyne derivative **8**.

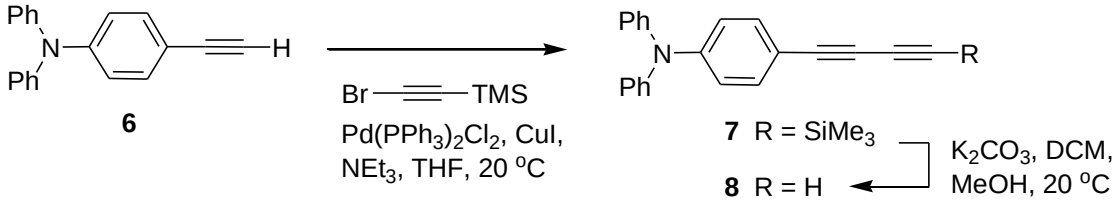

Compound **10** was obtained in 90% yield by bromination of **9** as shown in Scheme 2. Reactions of **10** with **6** and **8**, respectively, catalyzed by $Pd(PPh_3)_2Cl_2$ / CuI, under basic conditions gave the corresponding hexatriyne and octatetrayne products **3** and **4** in 56% and 39% yields. Scheme 3 shows the synthesis of compound **5**. Compound **12**[25] was converted into **13** for which the polar 2-hydroxy-2-propyl protecting group facilitated purification. Standard deprotection of **13** under basic conditions[26] gave the target alkyne reagent **14** (69% yield from the 2 steps). By analogy with the synthesis of **3**, the cross-coupling reaction of **14** with **10** gave **5** in 42% yield.

Scheme 2. Synthesis of compounds **3** and **4**.

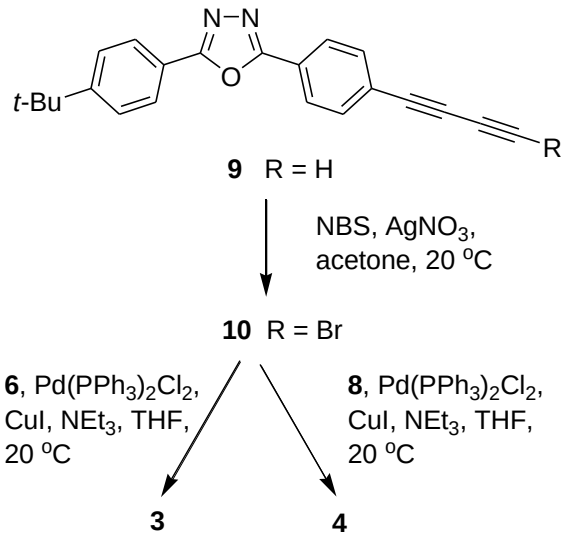

Scheme 3. Synthesis of compound **5**.

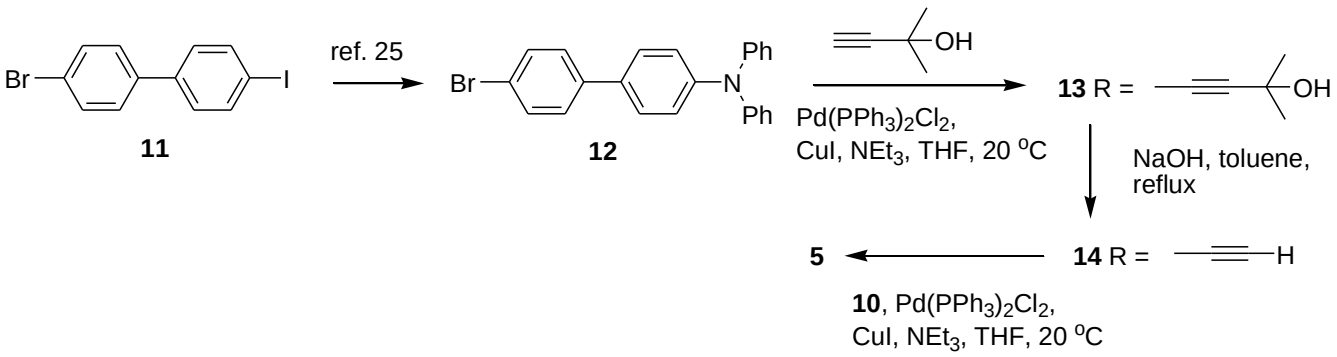

X-ray Crystallography. Single-crystal X-ray structures were determined for **3**, **4**, **5** (as a DCM hemi-solvate) and **8** (Figure 1). In each case, the N(3) atom has sp^2 geometry, with the three adjacent benzene rings inclined to its plane in a propeller-like fashion. The oligoyne 'rods' are substantially bent in **3** and **4** though not in **5**, the angle between the terminal C–C bonds amounting to 27.6º, 13.9º and 3.8º, respectively. Bonds in these moieties, as in other oligoynes,[19] alternate sharply between triple and single, and show no tendency to equalization. The butadiyne geometry in **8** is similar to those in recently

reported (surprisingly stable) terminal arylbutadiynes,[27] although the phenylene ring shows a slight quinoidal distortion.

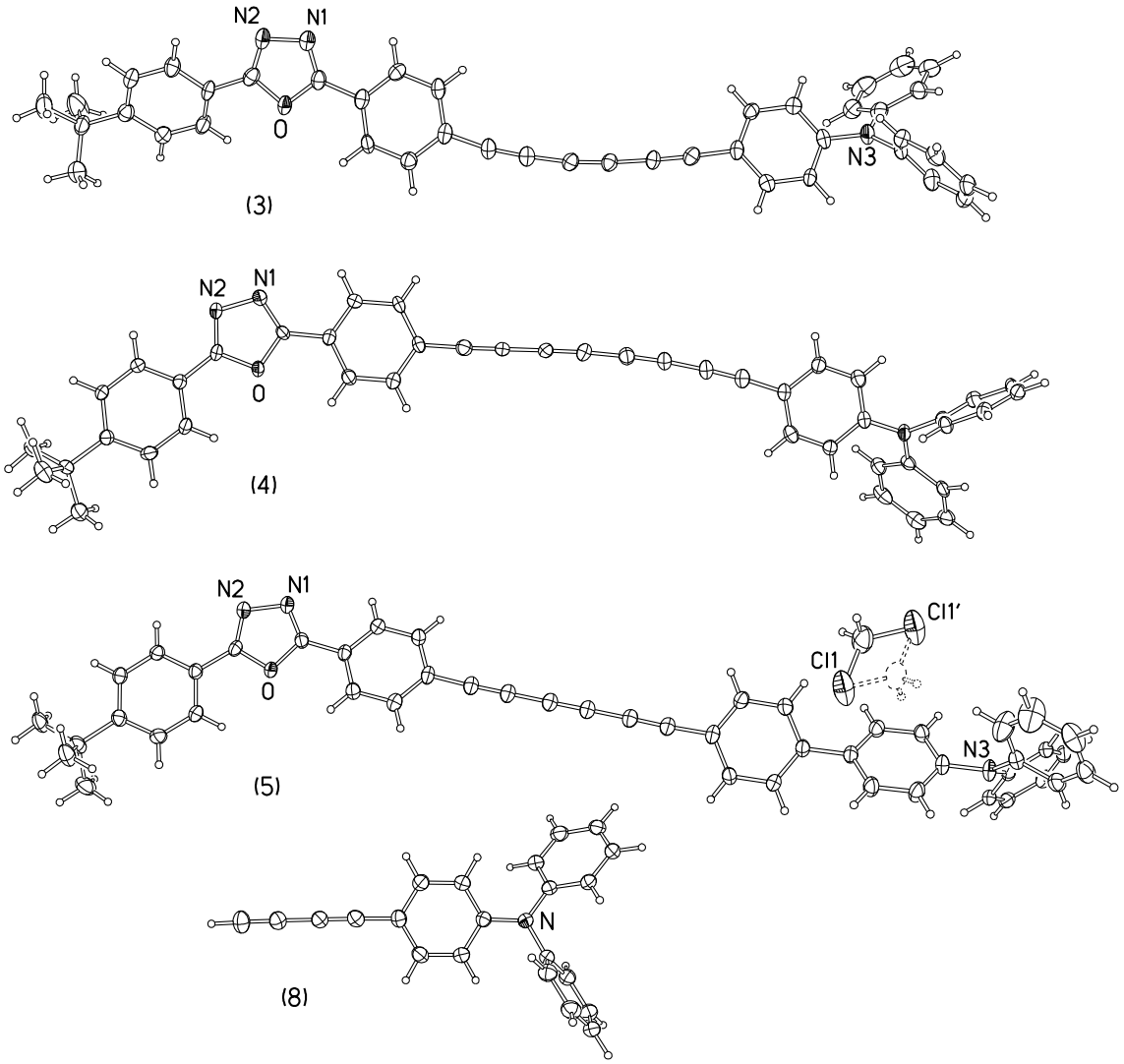

Figure 1. Molecular structures of **3**, **4**, **5**·½ CH_2Cl_2 and **8**, showing 50% thermal ellipsoids. Minor positions of the disordered DCM molecule and *t*-Bu group in **5** are omitted.

Solution electrochemistry. The solution redox properties of **1**,[23] **2**,[23] **3**, **4** and **5** have been studied by cyclic voltammetry (Figure 2). As expected, the CVs of these compounds are characterized by oxidation and reduction waves due to the triarylamine and oxadiazole moieties, respectively. These are irreversible waves except for the reduction of **1** which is quasi-reversible. In addition, for **2**-**5** irreversible reduction waves associated with the oligoyne bridges are observed at more negative potentials. The difference between the first oxidation and the first reduction potentials, $E^{ox1} - E^{red1}$, is a measure of the HOMO-

LUMO gap. A notable trend in Figure 3 is a reduction in the HOMO-LUMO gap in the series of compounds **1** – **4** as the oligoyne chain length increases, which is consistent with extended conjugation through the elongated bridges. A similar trend was noted in the CV data of two Zn-porphyrin–$(C{\equiv}C)_n$–C_{60} dyads (n = 1, 2) studied previously.[20] Interestingly, an increment of +30 to +50 mV in the value of E^{ox} was observed with each additional triple bond for compounds **1** – **4**. As noted previously for **1** and **2**,[23] and for some oligoyne-bridged binuclear organometallic compounds,[28,29] this can be ascribed to the electron-withdrawing nature of the extra triple bond. In the present D–$(C{\equiv}C)_n$–A systems we cannot exclude the possibility that charge delocalization across the bridge might play a role in causing these anodic shifts. Compound **5** has the lowest oxidation potential and this may be due to the biphenyl system interrupting conjugation into the electron-withdrawing oligoyne bridge. However, the irreversibility of the waves for **1**-**5** means that only tentative conclusions should be drawn from the CV data. It can be noted that there is a sequential decrease in the potential of the irreversible oxidation waves of the triarylamine building blocks **6**, **8** and **14** (see Supporting Information, Figure S1).

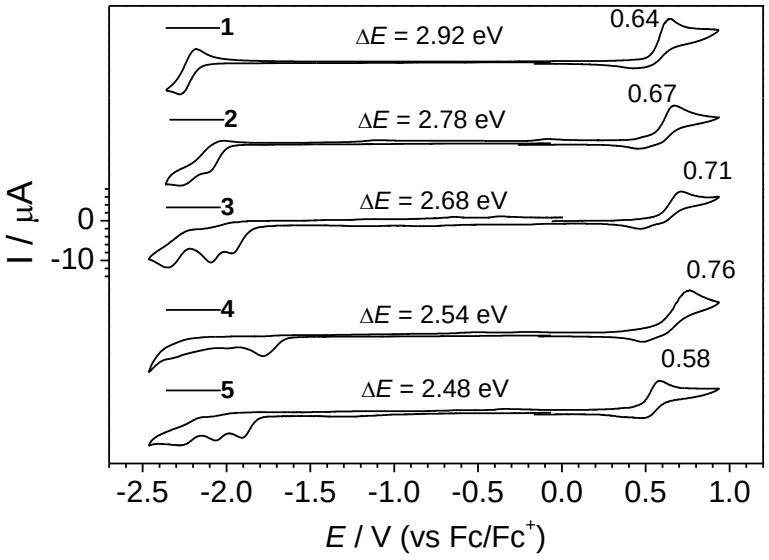

Figure 2. Cyclic voltammograms of compounds **1**-**5** in DMF. All of the solutions contained $TBAPF_6$ (0.1 M) as the supporting electrolyte, scan rate 100 mV/sec, using Pt disk (Φ 1.8 mm) as the working electrode, Pt wire as the counter electrode and $Ag/AgNO_3$-DMF as the reference electrode.

Photophysical studies.

Table 1 summarizes the absorption and emission data (when observed) and the Stokes shift (when observed) of **1 – 5** in methylcyclohexane (MCH) as obtained from the data shown for **1**, **2**, **3** and **5** shown in Figure 3. The data are extracted from the lowest energy absorption band (or shoulder) and the sharp peak in the emission spectra. The obtained Stokes shifts show a clear decrease as the conjugation is extended along the series from one to 3 alkyne units, i.e. compounds **1**, **2** and **3**, respectively. We note that this is likely to be an underestimate as different rotational conformations also contribute, as can be seen in the absorption spectra with underlying structures in for instance the absorption profile of **1** in MCH around ~26 000 cm^{-1}. The data does, however, imply that as the electronic system becomes more conjugated there is less displacement of the excited state potential energy curve relative to the ground state.

	$\tilde{\upsilon}_{abs}$ [cm^{-1}]	$\tilde{\upsilon}_{em}$ [cm^{-1}]	$\Delta\tilde{\upsilon}$ [cm^{-1}]	μ_g [D] AM1[c]	μ_g [D] PM3[c]	$\Delta\mu$ [D][b]	μ_e [D][d] AM1	μ_e [D][d] PM3
1	25575[a]	24570[a]	1005[a]	4.91	4.68	3.2 ± 0.1	8.1 ± 0.1	7.9 ± 0.1
2	24631[a]	23866[a]	764[a]	5.26	5.15	3.9 ± 0.2	9.2 ± 0.2	9.1 ± 0.2
3	23474[a]	22936[a]	538[a]	4.15	4.15	4.3 ± 0.3	8.5 ± 0.3	8.5 ± 0.3
4	21740[a]	-	-	4.27	4.64	-	-	-
5	24450[a]	22830	1620[a]	4.08	4.79	4.9 ± 0.3	9.0 ± 0.2	9.7 ± 0.2

Table 1. Data on the optical transitions of compounds **1-5**. [a] Recorded in a non-polar solvent (methylcyclohexane). $\Delta\tilde{\nu} = \tilde{\nu}_{abs} - \tilde{\nu}_{em}$. [b] $\Delta\mu$ according to equation 2. [c] AM1 and PM3 are the two semiempirical calculation methods used. The luminescence of **3** was recorded with relatively large slit widths (~ 10 nm) of the spectrometer. Accordingly, the center of weight of the luminescence is poorly defined which prevents an accurate calculation of the Stokes shift and thus $\Delta\mu$. [d] excited state dipole moment μ_e calculated from the ground state dipole moment and the difference dipole moment; $\mu_e = \mu_g + \Delta\mu$.

The efficiency of intramolecular charge transfer (ICT) in D–A dyads can be examined through optical absorption and emission experiments in media with different solvent polarity. In a low polarity solvent with a solvent density parameter of $\Delta f = 0$, where Δf is defined by equation (1):

$$\Delta f = \left(\frac{\varepsilon_r - 1}{2\varepsilon_r + 1} - \frac{n_D^2 - 1}{2n_D^2 + 1} \right) \quad (1)$$

where ε_r is the dielectric constant and n_D is the refractive index, the luminescence spectra of **1**, **2**, **3** and **5** in MCH (Figure 3) consist of two distinct features – a sharp and narrow band followed by a considerably broader and generally structure less component at lower energy. Interestingly, for all other solvents (dielectric medium) where $\Delta f > 0$, the narrow high energy component is no longer observed and the luminescence gives only a broader band devoid of any fine strcture. This is demonstrated in figure 3 which shows the photo luminescence (PL) in two different environments, MCH and toluene. With respect to equation 1, the solvent density parameter is $\Delta f = 0$ for MCH while for toluene $\Delta f = 0.013$. This observation indicates how sensitive the excited state is to the environment and how a very small change to more polar media will stabilize the charge transfer (CT) state. It is therefore cleat that for low polarity media with $\Delta f = 0$ the luminescence is due to two different contributions, namely a higher energy narrow band caused by singlet fluorescence ($\pi^* \rightarrow \pi$) and a broader lower energy intramolecular charge transfer (ICT) band. The existence of these two states was suggested by Khundkar et al[30] in studies of asymmetrically end-capped diphenylethyne and diphenylbutadiyne molecules – the singlet excited state has also been referred to as a locally excited (LE) state – although the LE state eluded detection in that study.

The hypothesis that the lower energy band is due to ICT is strengthened by absorption and emission experiments on the solvatochromism of **1**, **2**, **3** and **5**, using a number of solvents with varying polarity, as defined by the solvent density parameter (equation 1). The data give an apparent Stokes shift

$\Delta\tilde{\nu} = \tilde{\nu}_{\max}^{abs} - \tilde{\nu}_{\max}^{em}$, where the Stokes shift is now calculated from the lowest energy band in the absorption and the center of weight of the CT emission. Figure 4 shows the Stokes shift for **1**, **2**, **3** and **5** in various dielectric media. These experiments reveal that there is a moderate impact on the center of weight of the absorption while the luminescence center of weight is substantially more affected by the polarity of the medium. This in turn suggests that the ground state dipole moment is largely unaffected, in contrast to the excited state dipole moment which is considerably more sensitive to the medium. Semi empirical calculations (using two different methods, see Table 1) show that the ground state dipole moment is ca. 4 - 5 D and independent of the extent of conjugation, i.e. the number of alkyne units in the bridge. This, in turn, implies that when the D–A separation increases there is a slightly less charge localization in the ground state for the longer more conjugated compounds. The luminescence is, however, strongly dependent upon the properties of the dielectric medium and considerable bathochromic shifts of the PL center of weight with a more polar solvent are observed. The experimental observations were analyzed using the Lippert-Mataga-Oshika formalism (Equation 2).[31]

$$\Delta\tilde{\nu} = \tilde{\nu}_{\max}^{\mathrm{abs}} - \tilde{\nu}_{\max}^{\mathrm{em}} = \frac{2(\mu_e - \mu_g)^2}{hca^3}\left(\frac{\varepsilon_r - 1}{2\varepsilon_r + 1} - \frac{n_D^2 - 1}{2n_D^2 + 1}\right) + \text{constant} \qquad (2)$$

which relates the optical properties in various media to the difference dipole moment $\Delta\mu = \mu_e - \mu_g$ and the radius of the Onsager cavity, *a*. As shown in Figure 4, plots of the Stokes shift $\Delta\tilde{\nu}$ against the solvent density parameter Δf for all the compounds **1**, **2**, **3** and **5** results in a linear dependence as would be expected from the Lippert-Mataga-Oshika formalism. From the slope of the linear fits the difference dipole moment $\Delta\mu = \mu_e - \mu_g$ can be obtained from an estimate of the Onsager radius *a*. In estimating this radius we were guided by data from the crystal structures. From this selected bond distances and dihedral angles where obtained and using this information we estimated the Onsager radius. We acknowledge that assuming a spherical volume for these molecules is an approximation; however, we are not aware of any other way forward in this context.

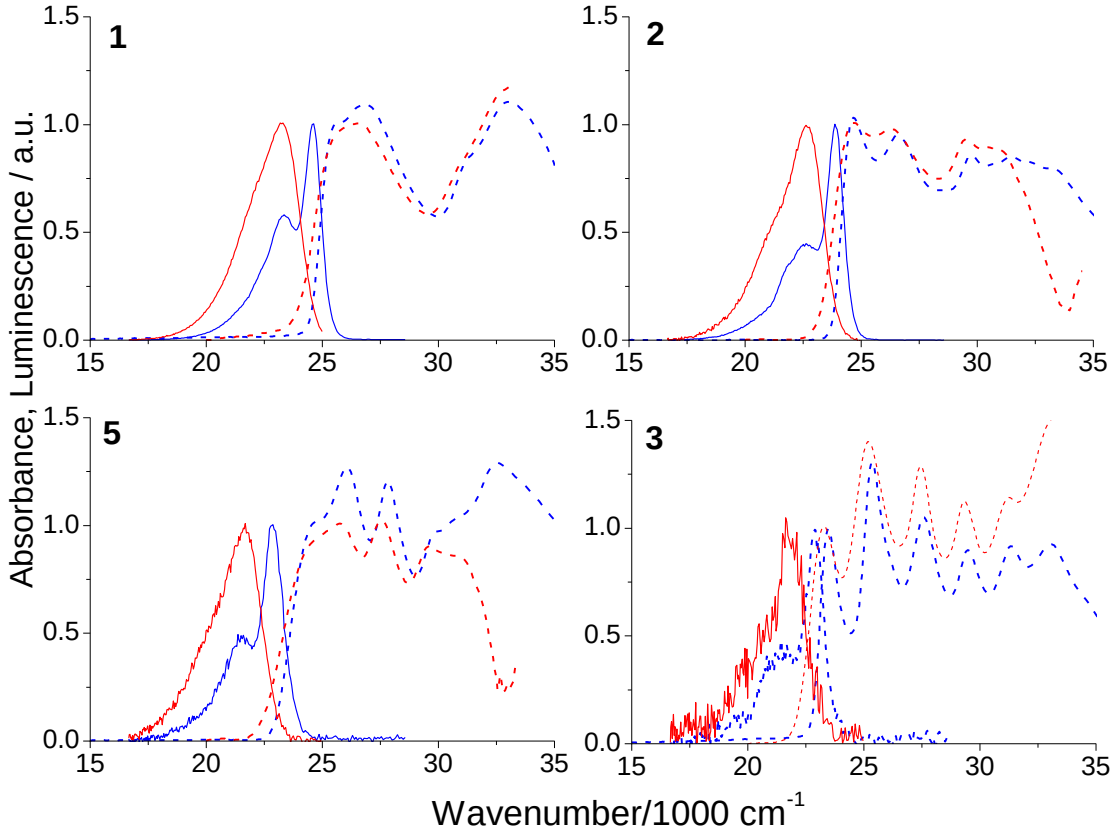

Figure 3. Absorption (dashed line) and luminescence (solid line) spectra for **1**, **2**, **3** and **5** in methylcyclohexane (blue) and toluene (red): excitation at 390 nm (25 641 cm^{-1}).

Interestingly, we find that that the difference dipole moment is larger for the more conjugated molecules **3** and **5**. This observation is in contrast to Stiegman et al. who observed a reduction in difference dipole moment for diphenylbutadiynyl D–π–A dyads [D–C_6H_4–$(C{\equiv}C)_n$–C_6H_4–A, n = 2] compared to diphenylethynyl analogs (n = 1).[32] This is significant as a relatively smaller excited dipole moment is indicative of less extensive ICT. We remark that the excited state dipole moments calculated here are in similar to the findings of Stiegman et al and appear to be typical for this type of D–A materials. The data obtained in the present study does, however, show that for these materials the ICT is equally efficient for the more conjugated longer compounds.

Khundkar et al. observed that when the ethynylene bridge was replaced by a butadiynylene bridge in compounds with the same donor and acceptor moieties [viz. MeS–C_6H_4–$(C{\equiv}C)_n$–C_6H_4–CN, n = 1, 2] there was a substantial reduction in the PLQY.[30b] The present series of compounds shows similar behavior with a dramatic drop in PLQY from 93% for **1** to 0.01 % for **3** (Table 2). Insertion of a phenyl ring in **5** results in a slight increase in PLQY although the value remains very low. We note that **4** appear to be luminescent, although the PLQY is extremely low, ca. 10^{-3}.

	PLQY[a]		σ_2 [GM]	
	MCH	Acetone	MCH	Acetone
1	0.93	0.56	50 ± 10	150 ± 10
2	0.36	0.28	140 ± 10	200 ± 10
3	0.01	0.01	190 ± 50	590 ± 100
4	~10^{-3}	-	-	-
5	0.04	-	-	-

Table 2. [a] PLQY values were measured in two different solvents based upon the absolute method using an integrating sphere. MCH is methylcyclohexane. Errors ± 5%. The TPA cross-sections were measured using fluorescein/NaOH as a standard (PLQY = 0.9 and σ_2 = 36 GM at λ_{exc} = 800 nm). The concentrations of the standard (fluorescein) was, $C^R = 5{\cdot}10^{-6}$ M and the concentration of the samples typically $C^S \approx 10^{-6}$ M. See SI for more information.

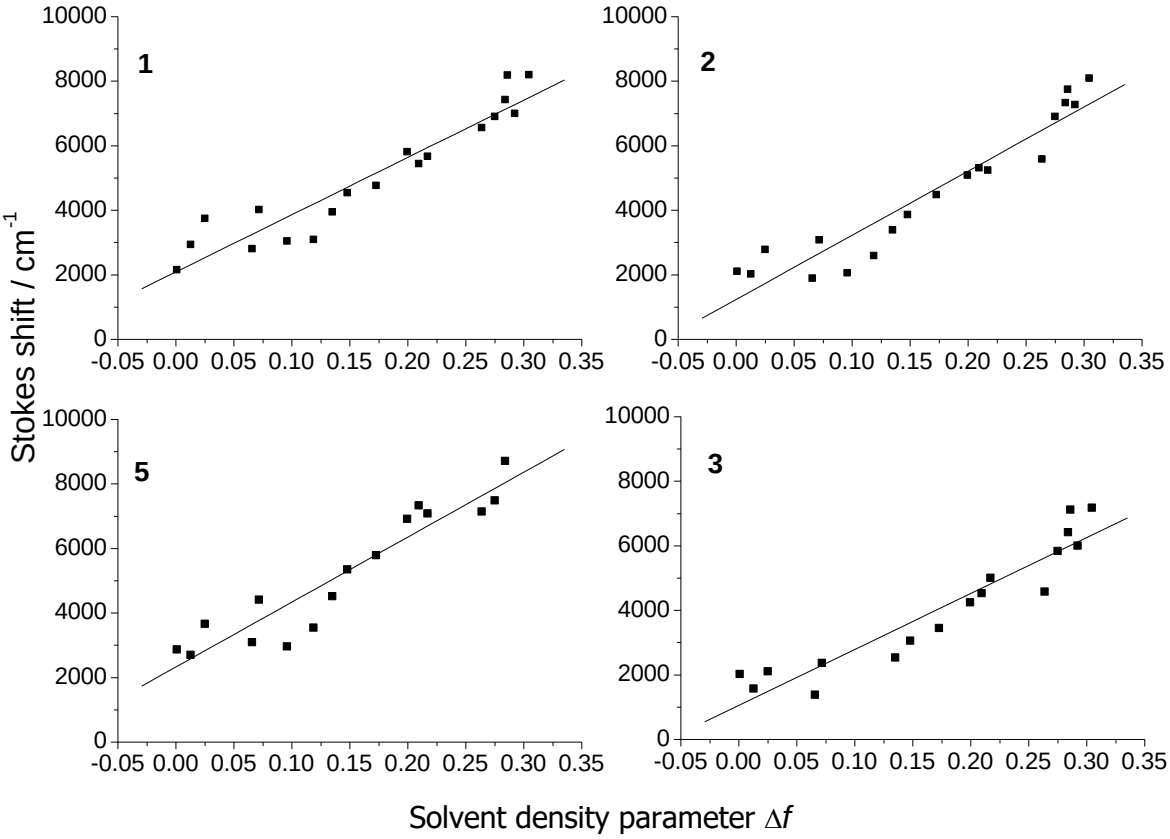

Figure 4. Stokes shifts for **1**, **2**, **3** and **5** as a function of solvent density parameter as defined in equation 1. The line represents a fit of the data according to the Lippert-Mataga-Oshika relationship as defined in equation 2 using a linear regression fit. The quality of the fit is judged by the corresponding *R* values which are as follows, for **1**; $R = 0.95$, **2**; $R = 0.96$, **3**; $R = 0.95$, **5**; $R = 0.94$.

To gain further insights into the optoelectronic properties we also performed two photon absorption (TPA) measurements on **1a**, **2** and **3**. Seminal work by Albota et al. clearly suggest that introduction of charge transfer moieties and extended conjugation of the π-electron system are prerequisites for high TPA cross-sections.[33] It was, therefore, most relevant to examine **1**, **2** and **3** in different dielectric media to assess the impact of conjugation within the homologous series. All three compounds exhibited clear and well-defined TPA PL for excitation at 790 nm, similar in shape to the corresponding linear one photon excited PL spectra with respect to center of weight of bands (see Figure S3). One difference that could be observed was that the relative intensity of the LE state emission (in methylcyclohexane) is slightly lower relative to the lower energy CT bands. This may be a reflection of different symmetry

implications of the TPA process. To examine the effect of changing the dielectric medium, the data for **1**, **2** and **3** were obtained in a non-polar solvent MCH ($\Delta f = 0$) and acetone ($\Delta f = 0.355$), which was the most polar medium in which the compounds were soluble. The data shown in Table 2 clearly show that the TPA cross-sections increase significantly for both **1** and **3** with increased polarity of the solvent. At present it is not clear why compound **2** shows a smaller relative increase in changing from a non-polar to a polar dielectric medium, compared to **1** and **3**. The polar solvents will stabilize the structure of the excited state in favor of a CT state over an LE state. This, in turn, has symmetry implications with possible conformation alterations, which explain the enhanced TPA cross-sections in polar media. In this context, it is necessary to make additional comments about the PLQY of these compounds. The data show that the PLQY is not only affected by conjugation (as previously discussed) but also by the properties of the dielectric medium. For **1** and **2**, there is a clear decrease of the PLQY in more polar media, as compared to MCH (Table 2). We remark that we observed a decrease in the PLQY relative to the PLQY in MCH for a number of other more polar solvents. However, there was no systematic variation of PLQY versus solvent density parameter (data not shown). The impact of the medium on **3** is more difficult to assess as the PLQY value is low. In parallel to the effect of the medium on the TPA cross-sections, there is also an effect due to increased conjugation. Compound **3**, with the more extended conjugation, also shows the largest TPA cross-sections, as expected.[33] (Note that although σ_2 for **3** is high, there is also a large associated error due to an uncertainty in the PLQY value, as previously discussed).

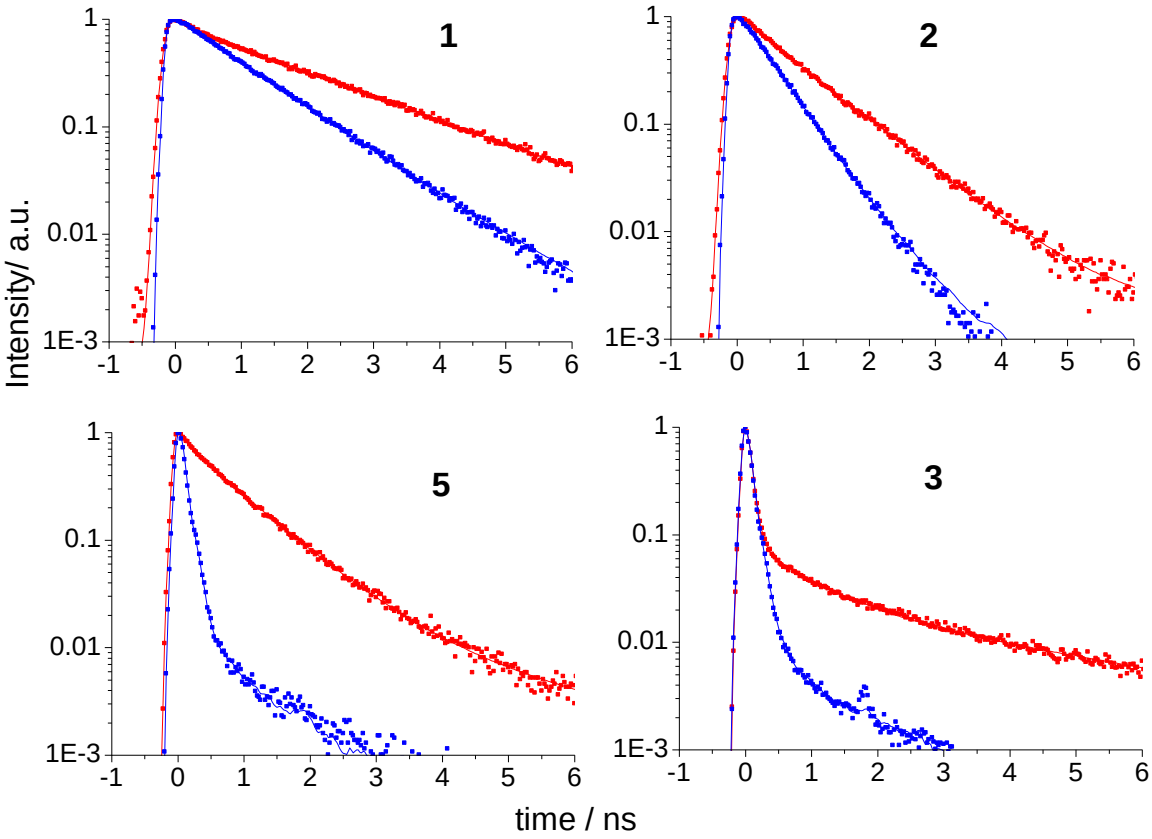

Figure 5. Luminescence decays recorded in the emission maxima of compounds **1**, **2**, **3** and **5**. Data recorded in polar solvent (chloroform: red) and a non-polar solvent (methylcyclohexane: blue). Excitation wavelength 295 nm. See text for details.

The luminescence decay of the excited state was also affected by the extent of conjugation through oligoyne bridging (Figure 5). For **1** in a non-polar medium the decay was dominated by a 1.1 ns component, while data for **2** was dominated by a ~500 ps component. For the more conjugated **3** and **5** the luminescence decay was very fast and most likely not fully resolved due to insufficient time-resolution of the detection system. Accordingly, the time constants for **3** and **5** (Table 3) are somewhat uncertain. In a polar environment a longer decay phase was observed for all four compounds. This supports the suggestion that the luminescence in polar media originates from an ICT state for which longer decay times are expected.[34] We note that the luminescence decays appear to be independent of the excitation wavelength. Essentially similar kinetics was obtained for excitation at 300 nm and 400 nm.

We also remark that there were only moderate variations of the PL dynamics with different detection wavelength (in the PL spectra), with the time resolution of our TCSPC apparatous. However, we can not rule the presence of PL decay phases in the 10^{-12} - 10^{-13} s range which would escape detection in our TCSPC system. In combination, the PLQY data and the luminescence decay data reveal that for the more conjugated systems **3** and **5** the excited state decay is dominated by non-radiative processes. Probing the excited state decay with transient absorption spectroscopy supports this conclusion. Figure 6 shows pump-probe absorption data for **1**, **2**, **3** and **4** in MCH at 390 nm after excitation with optical pulses with a temporal width of 200 fs.

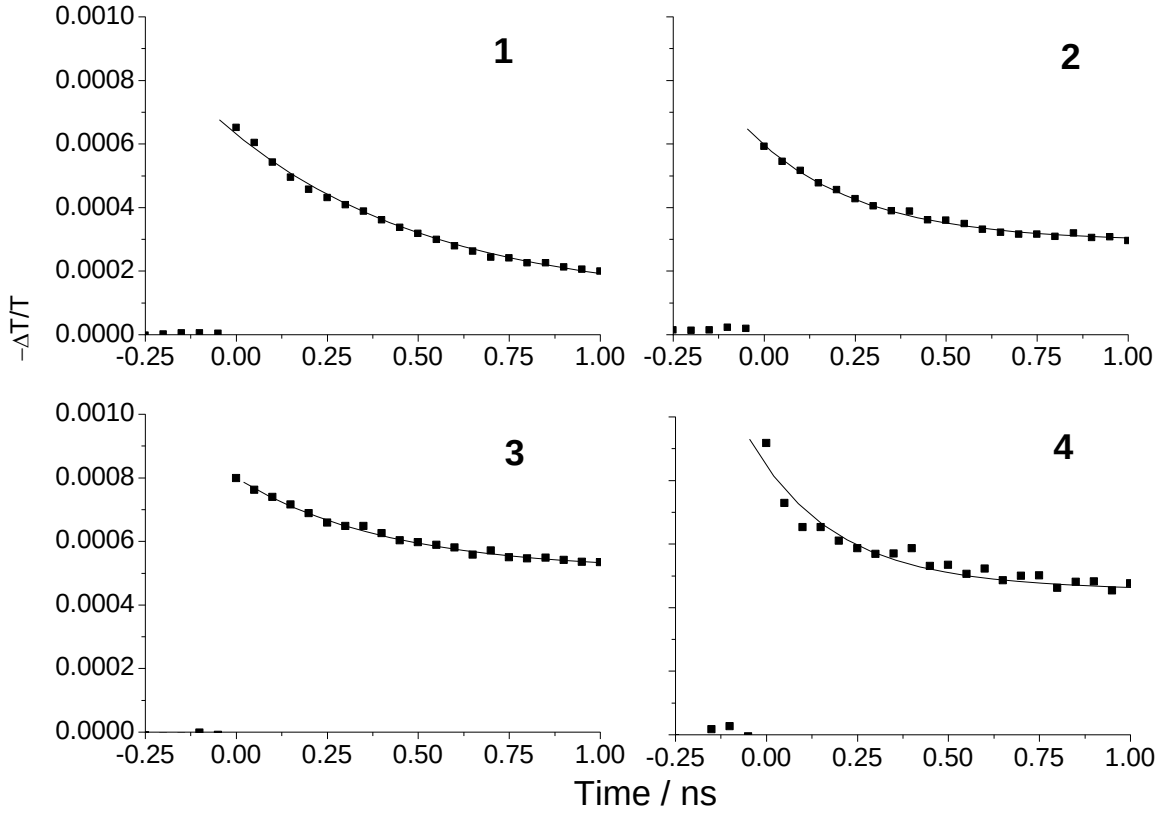

Figure 6. Ambient temperature transient absorption data for **1**, **2**, **3** and **4** for excitation and probing at 390 nm in MCH. The squares represent the measured data and the line is the fit of the data. See text for details.

All the systems studied have an initial fast decay to a longer-lived state which is estimated to have a lifetime of tens of ns. We note that there was no corresponding decay time found in the PL experiments. However, the same trend was observed in the ultrafast transient absorption as in the time-resolved PL experiments. This trend shows that the absorption recovery time of the first component becomes faster with increasing oligoyne bridging, i.e. increasing conjugation (see table 3). The PL dynamics is therefore limited by the excited state life time accordingly. The absorption excited state decay, as monitored in the transient absorption measurements, in a non-polar medium is due to two phases: a fast direct relaxation from the excited state to the ground state which limits the PL as stated previously, or via a charge separated state which will recombine non-radiatively on relatively slower timescales compared to the PL dynamics. In order to learn more about the nature of the slow ns component observed in the transient absorption measurements (Figure 6 and Table 3), additional experiments where performed on **3** and **4**, where this phase is more prominent. Excited state absorption experiments revealed a strong absorption at ca. 470 nm for both **3** and **4** (See SI for details). Probing the decay dynamics of this band at 470 nm did not result in any detected transient. The reason for this is the time-resolution of our experimental apparatus which is in the order of ~70 ns. Hence, the recovery in this band must in the ~10 ns range. Interestingly, when the probe wavelength was 639 nm a recovery to the ground state sufficiently slow that it could be monitored was observed. Furthermore, the decay dynamics of this species showed a marked sensitivity to the presence of oxygen. Hence we conclude that this absorption is due triplet-triplet absorption. It then remains to assign the strong band around 470 nm to excited state absorption of a dark charge transfer state with a lifetime in the ns regime as no corresponding decay phase was observed in the time-resolved PL experiments as previously mentioned.[35] This conclusion correlates well with the observation of fast luminescence dynamics observed for **3** (see Figure 5).

The initial faster decay shows interesting behavior depending on the length of the oligoyne bridge. This aspect will now be discussed in more detail. Compound **1**, with the shortest bridge, exhibits a slow

decay of the luminescence in conjunction with a slow return to the ground state in the transient absorption measurements. For more extended analogs **2**, **3** and **4** the kinetics become faster in both luminescence and transient absorption (Table 3). In conjunction with the PLQY data, the scenario is, therefore, that strong non-radiative pathways dominate the excited state decay for more conjugated systems. The same phenomena have been observed experimentally for a number of related systems.[36] The mechanism behind the non-radiative decay has not yet been clarified but the possibility that the non-radiative relaxation is connected to the ground and excited state energy gap has been considered.[36] This dependency is commonly known as the energy-gap law and the framework was outlined by Engelman and Jortner in the 1970s.[24] This law defines two limiting cases, referred to as the strong and weak coupling limits, which in turn relate to the extent of displacement of the LUMO relative to the HOMO potential energy surface. In the case of the weak coupling limit, the reorganization energy (λ) is considered to be small and it also assumes a moderate temperature dependence of the PLQY, which was observed for the present series of compounds (see SI for details). Prominent factors in the weak coupling limit are high frequency vibrational modes which are common for organic-based materials. For the strong coupling limit on the other hand, the potential surfaces of the ground and excited state are identical. The strong coupling case implies that the Stokes shift considerably exceeds the mean vibrational frequency.[24] From the recorded Stokes shifts (Table 1) we conclude that those are likely significantly less than the energies of prominent vibrational modes of the systems studied here.

Assuming that the weak coupling limit is valid in this case, the non-radiative decay rate is then given by equation (3):[36]

$$k_{nr} = \frac{V^2 (2\pi)^{\frac{1}{2}}}{\hbar (\hbar\omega_M \Delta E)^{\frac{1}{2}}} \cdot \exp\left[-\frac{\lambda}{\hbar\omega_M}\right] \cdot \exp\left[-\frac{\gamma \Delta E}{\hbar\omega_M}\right] \qquad (3)$$

In this formalism V is the electronic coupling between the ground and excited state and ΔE energy gap (LUMO – HOMO) and ω_M is the vibrational frequency. The reorganization energy, λ, must be equal to,

or less than, the average vibrational energy; $\hbar\omega_{ave}$ and for the systems studied here prominent modes are the ~1600 cm^{-1} C=C stretch; also the C≡C stretch ~2200 cm^{-1} and the –C-H- stretch ~3000 cm^{-1} are important modes. We remark that the energy in both these vibrations exceeds the reorganization energy as estimated from the Stokes shift obtained from the lowest energy band in the absorption spectra and the sharp LE emission (see Figure 1 and Table 1).

In equation 3 the parameter γ depends only weakly on the energy gap ΔE and the analytical expression for γ is given by equation (4):[36]

$$\gamma = \ln\left(\frac{2\Delta E}{n\hbar\omega_M \Delta Q^2}\right) - 1 \tag{4}$$

where ΔQ is the average displacement between the ground and excited state potential energy surfaces. Taking the natural logarithm of equation 3 will give equation (5).

$$\ln k_{nr} \propto -\frac{1}{2}\ln \Delta E - \gamma \frac{\Delta E}{\hbar\omega_M} \tag{5}$$

This is more useful as there is a linear relationship between ln k_{nr} and ΔE. Furthermore, the logarithmic term in equation 5 contributes only marginally to the dependence of ΔE on ln k_{nr}. Consequently, the pre-exponential factor in equation (3) can be regarded as a constant and with these approximations the relationship in equation (6) is obtained where C is the constant term:

$$\ln k_{nr} \approx C \cdot \gamma \frac{\Delta E}{\hbar\omega_M} \tag{6}$$

	Lum. decay (MCH)[a]		Lum. decay ($CHCl_3$)[b]		Pump-probe abs. (MCH)[a]		ΔE [eV]
	τ_1 (ns)	τ_2 (ns)	τ_1 (ns)	τ_2 (ns)	τ_1 (ns)	τ_2 (ns)	
1	1.0	-	0.2 (10%)	2.0 (90%)	0.78	-	3.17
2	0.5	-	0.1 (5%)	1.0 (95%)	0.35 (50%)	~15 (50%)	3.05
3	~0.06	-	0.1 (5%)	1.0 (95%)	0.30 (50%)	~10(50%)	2.91
4	-	-	-	-	0.03 (50%)	~10(50%)	2.71
5	~0.06	-	0.15 (5%)	1.0 (95%)	-	-	-

Table 3. Data obtained in time domain experiments. Luminescence decay data were obtained in TCSPC experiments. [a] MCH: methylcyclohexane. [b] chloroform. Percentage number in brackets is the relative contribution of the particular decay phase. The energy gap is taken as the lowest energy absorbing species in the absorption spectrum. See text for details.

Figure 7 displays the results obtained for compounds **1**, **2**, **3** and **4** where the length of the oligoyne bridge is systematically extended. The data fit reasonably well to a linear dependence, as would be expected from equation (6) and thus confirms a weak coupling behavior as outlined previously.

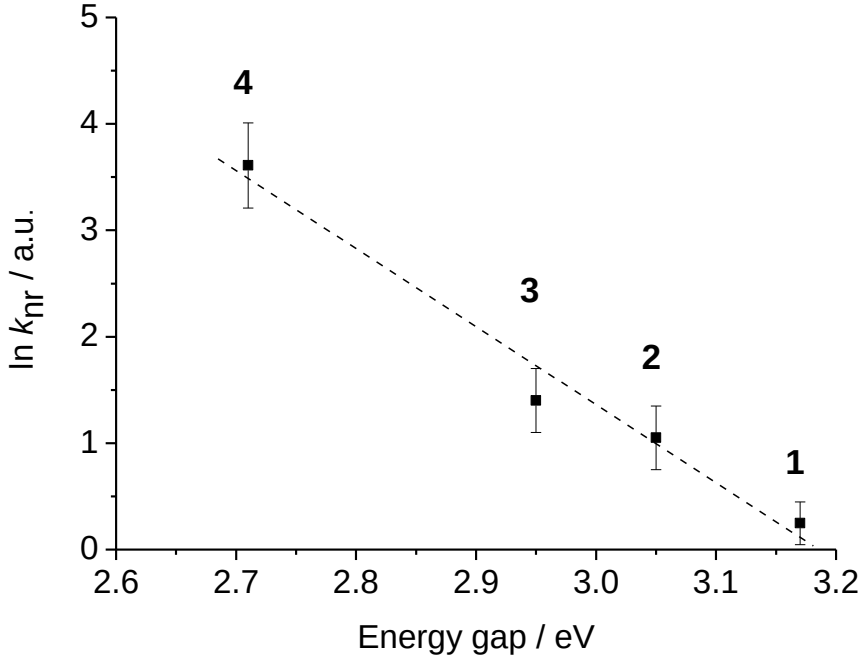

Figure 7. The non-radiative decay rates for **1**, **2**, **3** and **4** plotted against the energy gap**.** The dashed line indicates a linear trend of the data. See text for details.

Conclusions

We have observed strong solvatochromism of the photoluminescence (PL) which points to an efficient intramolecular charge transfer, even for the longer, more conjugated dyads. Two photon excitation (TPE) PL lends support to this hypothesis as the TPE cross-section was found to be sensitive to the properties of the dielectric medium and the extent of conjugation. The PLQY was observed to be extremely dependent upon the size of the conjugated π-electron system as well as the PL decay. This phenomenon has been observed previously for a number of similar systems, but the origin of this effect was not clearly established.[30] By investigating the excited state properties of the series of triphenylamine–$(C{\equiv}C)_n$–oxadiazole dyads we have shown that the initial fast excited state decay is governed by the electronic energy gap law as formulated by the Engelman – Jortner model. For the present series of dyads we observe intramolecular charge transfer and have established that the non-radiative decay is driven by the weak coupling limit. This contrasts with the Zn-porphyrin–$(C{\equiv}C)_n$–C_{60} dyads (n = 1-4)[20] which possess stronger electron donor and acceptor moieties and exhibit classical Marcus behavior, i.e. electron transfer with a very small attenuation factor (β). The present study is among the most comprehensive reported to date on the optoelectronic properties of oligoyne bridged molecular wires and should stimulate further work on electronic interactions mediated by these fascinating π–electron bridges.

Acknowledgements. C.S.W. was funded by EPSRC. L.O.P. acknowledges financial support from CENAMPS. We thank Professor J. A. K. Howard for the use of X-ray facilities and EPSRC for funding the improvement to the X-ray instrumentation.

Supporting Information Available. General experimental methods, synthetic details and characterization data for **3**-**5**, **7**, **8**, **10**, **13** and **14**; additional photophysical data; X-ray crystallographic file for **3**, **4**, **5** and **8** in CIF format. This material is available free of charge via internet at http://pubs.acs.org

† Department of Chemistry.

‡ Department of Physics.

(1) (a) *Electron Transfer in Chemistry* (Ed. Balzani, V.), Wiley-VCH, Weinheim, 2001. (b) Adams, D. M.; Brus, L.; Chidsey, C. E. D.; Greager, S.; Creutz, C.; Kagan, C. R.; Kamat, P. V.; Lieberman, M.; Lindsay, S.; Marcus, R. A.; Metzger, R. M.; Michel-Beyerle, M. E.; Miller, J. R.; Newton, M. D.; Rolison, D. R.; Sankey, O.; Schanze, K. S.; Yardley, J.; Zhu, X. *J. Phys. Chem. B* **2003**, *107*, 6668-6697. (c) Weiss, E. A.; Wasielewski, M. R.; Ratner, M. A. *Top. Curr. Chem*. **2005**, *257*, 103-133.

(2) Reviews on molecular electronics: (a) Carroll, R. L.; Gorman, C. B. *Angew. Chem. Int. Ed*. **2002**, *41*, 4378-4400. (b) Benniston, A. C. *Chem. Soc. Rev*. **2004,** *33,* 573-578. (c) Maruccio, G.; R. Cingolani, R.; Rinaldi, R. *J. Mater. Chem*. **2004**, *14*, 542-554. (d) Troisi, A.; Ratner, M. A. *Small* **2006**, *2*, 172-181.

(3) (a) Oevering, H.; Paddon-Row: M. N.; Heppener, M.; Oliver, A. M.; Cotsaris, E.; Verhoeven, J. W.; Hush, N. S. *J. Am. Chem. Soc.* **1987**, *109*, 3258-3269. (b) Wasielewski, M. R. *J. Org. Chem.* **2006**, *71*, 5051-5066.

(4) Review: Albinsson, B.; Eng, M. P.; Pettersson, K.; Winters, M. U. *Phys. Chem. Chem. Phys*. **2007**, *9*, 5847–5864.

(5) (a) Low, P. J. *Dalton Trans*. **2005**, 2821-2824. (b) Benniston, A. C.; Harriman, A. *Coord. Chem. Rev*. **2008**, *252*, 1268-1277.

(6) *Electronic Materials*: *The Oligomer Approach*; Wegner, G., Müllen, K., Eds.; Wiley-VCH: Weinheim, Germany, 1998.

(7) (a) Giacolone, F.; Segura, J. L.; Martín, N.; Guldi, D. M. *J. Am. Chem. Soc.* **2004***, 126,* 5340-5341.

(8) (a) Benniston, A. C. *Chem. Soc. Rev*. **2004**, *33*, 573-578. (b) Irie, M. *Chem. Rev*. **2000**, *100*, 1685-1716. (c) Gust, D.; Moore, T. A.; Moore, A. L. *Chem. Commun*. **2006**, 1169-1178. (d) Balzani, V.; Credi, A.; Venturi, M. *Molecular Devices and Machines,* Wiley-VCH: Weinheim, Germany, 2008.

(9) Günes, S.; Neugebauer, H.; Sariciftci, N. S. *Chem. Rev*. **2007**, *107*, 1324-1338.

(10) Shirota, Y.; Kageyama, H. *Chem. Rev*. **2007**, *107*, 953-1010.

(11) Zaumseil, J.; Sirringhaus, H. *Chem. Rev*. **2007**, *107*, 1296-1323.

(12) (a) McCreery, R. L. *Chem. Mater*. **2004**, *16*, 4477–4496. (b) Lindsay S. M.; Ratner, M. A. *Adv. Mater*. **2007**, *19*, 23–31. (c) Chen, F.; Hihath, J.; Huang, Z.; Li, X.; Tao, N. J. *Annu. Rev. Phys. Chem*. **2007**, *58*, 535–564.

(13) Weiss, E. A.; Ahrens, M. J.; Sinks, L. E.; Gusev, A. V.; Ratner, M. A.; Wasielewski, M. R. *J. Am. Chem. Soc.* **2004**, *126*, 5577-5584.

(14) (a) Segura, J. L.; Martín, N.; Guldi, D. M. *Chem. Soc. Rev.* **2005**, *34*, 31–47. (b) Giacalone, F.; Segura, J. L.; Martín, N.; Ramey, J.; Guldi, D. M. *Chem. Eur. J*. **2005**, *11*, 4819 – 4834.

(15) (a) Bunz, U. H. F. *Chem. Rev*. **2000**, *100*, 1605-1644. (b) Atienza, C.; Insuasty, B.; Seoane, C.; Martín, N.; Ramey, J.; Rahman, G. M. A.; Guldi, D. M. *J. Mater. Chem*. **2005**, *15*, 124-132. (c) Atienza, C.; Martín, N.; Wielopolski, M.; Haworth, N.; Clark, T.; Guldi, D. M. *Chem. Commun*. **2006**, 3202-3204. (d) Pettersson, K.; Wiberg, J.; Ljungdahl, T.; Martensson, J.; Albinsson, B. *J. Phys. Chem. A* **2006**, *110*, 319-326.

(16) (a) Goldsmith, R. H.; Sinks, L. E.; Kelley, R. F.; Betzen, L. J.; Liu, W.; Weiss, E. A.; Ratner, M. A.; Wasielewski, M. R. *Proc. Natl. Acad. Sci. U. S. A.* **2005**, *102*, 3540-3545. (b) Atienza-Castellanos, C.; Wielopolski, M.; Guldi, D. M.; van der Pol, C.; Bryce, M. R.; Filippone, S.; Martín, N. *Chem. Commun*. **2007**, 5164-5166. (c) Goldsmith, R. H.; DeLeon, O.; Wilson, T. M.; Finkelstein-Shapiro, D.; Ratner, M. A.; Wasielewski, M. R. *J. Phys. Chem. A* **2008**, *112*, 4410-4414.

(17) Otsubo, T.; Aso, Y.; Takimiya, K. *J. Mater. Chem*. **2002**, *12*, 2565-2575.

(18) (a) Arrhenius, T. S.; Blanchard-Desce, M.; Dvolaitzky, M.; Lehn, J. M.; Malthete, J. *Proc. Natl. Acad. Sci. U.S.A.* **1986**, *83*, 5355-5359. (b) Díaz, M. C.; Herranz, M. A.; Illescas, B. M.; Martín, N.; Godbert, N.; Bryce, M. R.; Luo, C.; Swartz, A.; Andersen, G.; Guldi, D. M. *J. Org. Chem*. **2003**, *68*, 7711-7721. (c) He, F.; Chen, F.; Li, J.; Sankey, O. F.; Terazono, Y.; Herrero, C.; Gust, D.; Moore, T. A.; Moore, A. L.; Lindsay, S. M. *J. Am. Chem. Soc*. **2005**, *127*, 1384-1385. (d) Akemann, W.; Laage, W.; Plaza, P.; Martin, M. M.; Blanchard-Desce, M. *J. Phys. Chem. B*. **2008**, *112*, 358-368.

(19) (a) Szafert, S.; Gladysz, J. A. *Chem. Rev*. **2003**, *103*, 4175-4205. (b) Szafert, S.; Gladysz, J. A. *Chem. Rev*. **2006**, *106*, PR1-PR33. (c) Gibner, T.; Hampel, F.; Gisselbrecht, J. P.; Hirsch, A. *Chem. Eur. J*. **2002**, *8*, 408-432. (d) Morisaki, Y.; Luu, T.; Tykwinski, R. R. *Org. Lett*. **2006**, *8*, 689-692. (e) Kendall, J.; McDonald, R.; Ferguson, M. J.; Tykwinski, R. R. *Org. Lett*. **2008**, *10*, 2163-2166.

(20) Vail, S. A.; Krawczuk, P. J.; Guldi, D. M.; Palkar, A.; Echegoyen, L.; Tomé, J. P. C.; Fazio, M. A.; Schuster, D. I. *Chem. Eur. J*. **2005**, *11*, 3375-3388.

(21) (a) Taylor, J.; Brandbyge, M.; Stokbro, K. *Phys. Rev. B*, **2003**, *68,* 121101. (b) James, P. V.; Sudeep, P. K.; Suresh, C. H.; Thomas, K. G. *J. Phys. Chem. A* **2006**, *110*, 4329-4337.

(22) (a) Slepkov, A. D.; Hegmann, F. A.; Eisler, S.; Elliott, E.; Tykwinski, R. R. *J. Chem. Phys. B* **2004**, *15,* 6807-6810. (b) Eisler, S.; Slepkov, A. D.; Elliott, E.; Luu, T.; McDonald, R.; Hegmann, F. A.; Tykwinski, R. R. *J. Am. Chem. Soc*. **2005**, *127*, 2666-2676.

(23) Wang, C.; Pålsson, L.-O.; Batsanov, A. S.; Bryce, M. R. *J. Am. Chem. Soc.* **2006**, *128*, 3789-3799.

(24) (a) Engelman, R.; Jortner, J. *J. Mol. Phys.* **1970**, *18,* 145-164, (b) Freed, K. F.; Jortner, J. *J. Chem. Phys.* **1970**, *52,* 6272-6291.

(25) Gauthier, S.; Frechet, J. M. J. *Synthesis* **1987**, 383-385.

(26) (a) Ames, D. E.; Bull, D.; Takunda, C. *Synthesis* **1981**, 364–365. (b) Novák, Z.; Nemes, P.; Kotschy, A. *Org. Lett.* **2004**, *6,* 4917–4920.

(27) (a) West, K.; Wang, C.; Batsanov, A. S.; Bryce, M. R. *J. Org. Chem*. **2006**, *71*, 8541-8544. (b) West, K.; Wang, C.; Batsanov, A. S.; Bryce, M. R. *Org. Biomol. Chem*. **2008**, *6*, 1934-1937. (c) West, K.; Hayward, L. N.; Batsanov, A. S.; Bryce, M. R. *Eur. J. Org. Chem*. **2008**, 5093-5098. (d) Wang, C.; Batsanov, A. S.; West, K.; Bryce, M. R. *Org. Lett*. **2008**, *10*, 3069-3072.

(28) Xu, G.-L.; Wang, C.-Y.; Ni, Y.-H.; Goodson III, T. G.; Ren, T. *Organometallics* **2005**, *24*, 3247-3254.

(29) For analysis of the redox properties of symmetrical organometallic-capped oligoyne chains see: (a) Brady, M.; Weng, W.; Zhou, Y.; Seyler, J. W.; Amoroso, A. J.; Arif, A. M.; Böhme, M.; Frenking, G.; Gladysz, J. A. *J. Am. Chem. Soc.***1997**, *119*, 775-788. (b) Dembinski, R.; Bartik, T.; Bartik, B.; Jaeger, M.; Gladysz, J. A. *J. Am. Chem. Soc*. 2000, *122*, 810-822.

(30) (a) Khundkar, L. R.; Bartlett, J. T; Biswas, M. *J. Chem. Phys.* **1995**, *102*, 6456-6462. (b) Biswas, M.; Nguyen, P.; Marder, T. B.; Khundkar, L. R. *J. Phys. Chem. A* **1997**, *101*, 1689-1695, (c) Il'chev, Y. V.; Kühle, W.; Zachariasse, K. A. *J. Phys. Chem. A* **1998**, *102*, 5670-5680. (d)

Zachariasse, K. A.; van der Haar, T.; Hebecker, A.; Leinhos, U.; Kühle, W. *Pure & Appl. Chem*. **1993**, *65*, 1745-1750.

(31) (a) Oshika, Y. *J. Phys. Soc. Jpn.* **1954**, *9*, 594-601. (b) Lippert, E. Z. *Naturforschung* **1955**, *10a*, 541-545. (c) Mataga, N.; Kaifu, Y.; Koizumi, M. *Bull. Chem. Soc. Jpn.* **1956**, *29*, 465-470.

(32) Stiegman, A. E.; Graham, E.; Perry, K. J.; Khundkar, L. R.; Cheng, L.-T.; Perry, J. W. *J. Am. Chem. Soc*. **1991**, *113,* 7658-7666.

(33) Albota, M.; Beljonne, D.; Brédas J.-L.; Ehrlic, J. E.; Fu, J.-Y.; Heikal, A.A.; Hess, S. E.; Kogej, T.; Levin M. D.; Marder S. M.; McCord-Maughon, D.; Perry, J. W.; Röckel, H.; Rumi, M.; Subramaniam, S.; Webb, W. W.; Wu, X.-L.; Xu, C. *Science* **1998**, *281*, 1653-1656.

(34) Dias, F. B.; Pollock, S.; Hedley, G.; Pålsson L.-O.; Monkman, A. P.; Perepichka, I. I.; Perepichka, I. F.; Tavasli, M.; Bryce, M. R. *J. Phys. Chem. B* **2006**, *110*, 19329-19339.

(35) Khundkar, L. R.; Stiegman, A. E.; Perry, J. W. *J. Phys. Chem*. **1990**, *94*, 1224-1226.

(36) (a) Bixon M.; Jortner, J.; Cortes, J.; Heltele, H.; Michel-Beyerle, M. E. *J. Phys. Chem*. **1994**, *98*, 7289-7299. (b) Andersson, P. O.; Bachilo, S. M.; Chen, R.-L.; Gillbro, T. *J. Chem. Phys*. **1995**, *99*, 16199-16209.

Table of contents graphic

Efficient Intramolecular Charge Transfer in Oligoyne-Linked D–π–A Molecular Wires

Lars-Olof Pålsson,* Changsheng Wang, Andrei S. Batsanov, Simon M. King, Andrew Beeby, Andrew P. Monkman and Martin R. Bryce*